# New collimating shielded bellow for the connection of superconducting rf cavities in a high current storage ring

H.-W. Glock,* V. Dürr, F. Glöckner, M. Ries, E. Sharples-Milne, M. Tannert, D. Wolk, A. Velez,† and J. Knobloch‡

*Helmholtz-Zentrum Berlin für Materialien und Energie, 14109 Berlin, Germany*

(Received 18 January 2023; accepted 3 April 2023; published 24 April 2023)

The implementation of concatenated superconducting rf cavities into high current storage rings raises the demand for appropriate beam pipe bellows. In order to compensate for length variations of the cavities due to thermal shrinkage and tuning, a mechanically soft element is required. It also should be of the least interaction with the beam to reduce the deposition of electromagnetic field energy, i.e., wakefields. Even in close neighborhood to high level cavity fields, parasitical Ohmic losses need to be minimized in order not to exceed cryogenic cooling capabilities. Overall construction length is an issue since real estate is strongly limited in between the existing magnetic lattice. The device needs to be compatible with cryogenic and ultrahigh vacuum conditions. The paper describes such a device as it was developed and tested in the framework of the Variable pulse length Storage Ring (VSR) Demo project, pursued at Helmholtz-Zentrum Berlin as a possible upgrade of the synchrotron light source BESSY II. It is denoted as Collimating Shielded Bellow, named such since it furthermore acts as an actively cooled synchrotron light collimator. The mechanical, electrodynamical, and thermal designs are presented. Particular attention is paid to the testing setup and the vacuum performance with the beam observed during extended testing periods in BESSY II.

DOI: 10.1103/PhysRevAccelBeams.26.043201

## I. INTRODUCTION

The paper details the design, development, and testing of a new device, denoted as a collimating shielded bellow (abbreviated as CSB), in particular its requirements, its electrodynamical, thermal, and mechanical design, the setup and results of the beam test of its first design (CSB1), the design updates included in its second generation (CSB2), and the outcomes from the second period of testing with beam in the synchrotron light source BESSY II. In order to set the context for the present work, this introduction starts in Sec. I. A with a brief description of the VSR/VSR DEMO project. In Sec. I. B, the technical demands for the CSB are summarized and other possible approaches are compared. In Sec. I. C, the structure of the following chapters is explained, both in view of the main technological reasons and some chronology of the development.

### A. VSR and VSR DEMO

Bunch length modulation for the simultaneous storage of longer high-charge (as foreseen 1.32 nC, 15 ps rms length) and ultrashort lower-charge bunches (0.14 nC, 1.1 ps rms length) would increase the versatility of BESSY II up to a level not yet reached by any other light source [1,2], especially if this mode can be effortless chosen alternatively to the proven standard operation modes.

Such an operation, denoted as VSR could become real using a module with four superconducting rf (SRF) cavities, intended to heavily modulate the accelerating electric field that acts on the circulating electron bunches (see Ref. [2] for details). Those cavities are designed with one coaxial fundamental power coupler plus five waveguide-connected higher-order mode (HOM) loads in order to accommodate the kW-scale wake power generated by the 300 mA of beam current [3].

To achieve alternating bunch length modulation, two cavities need to operate at the third harmonic frequency of the basic rf frequency of (close to) 500 MHz, used in the normal conducting accelerating cavity system of BESSY II, which is 1.5 GHz. Two more cavities have to oscillate with the 3.5th harmonic frequency, i.e., 1.75 GHz.

The SRF cavities are cooled down to 1.8 K by immersion into superfluid liquid helium (LHe). Operation under these conditions poses a variety of technical challenges, explained in Ref. [3]. To investigate the best way to deal

*hans.glock@helmholtz-berlin.de
†Also at Technical University Dortmund, Dortmund, Germany.
‡Also at University of Siegen, Siegen, Germany.

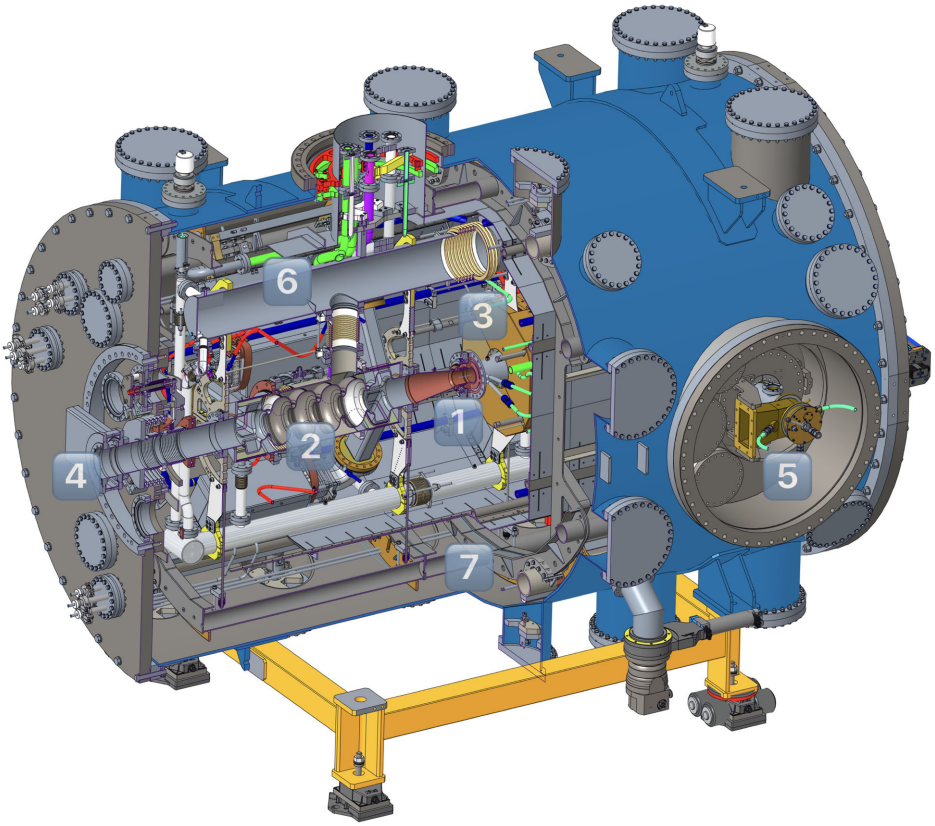


FIG. 1. The VSR DEMO module construction [4] has recently been built. The CSB ((1) brown, half cut) is located in the middle of two 1.5-GHz SRF cavities (upstream one (2) shown cut, downstream one hidden in its magnetic shield (3)). Further elements among others are the upstream beam pipe entry (4), the downstream fundamental power connection (5), the He gas return pipe (6), and the supporting space frame (7).

with these specific technological demands, VSR DEMO (cf. Fig. 1) is currently under construction with the aim to demonstrate a beam-ready two-cavity-module combining almost all the technology needed for a full VSR setup. In this context, the project needs the development of a one-of-a-kind component, which is the object of this work, to function as a bellow in the middle of the module while also fulfilling the many specifications as described in the following section (cf. Fig. 1).

### B. General CSB construction, aims, and restrictions

#### *1. Mechanical flexibility*

Mechanical flexibility is obviously the most fundamental property of beam pipe bellows. They are needed for the beam pipe connection between superconducting cavities since those operate with extremely small rf bandwidths. That makes their tuning highly sensitive against any deformations caused by external forces, which would be generated in case of stiff connections by the following five reasons (here in particular for the parameters of the VSR cavities):

*Thermal shrinkage* reduces the length of each cavity by about 1.1 mm when cooled down from room temperature to the 1.8-K operating temperature. This must be compensated for to allow for the externally connected fundamental power coupler of each cavity [5] to keep its position. To do so, at least one compensating element per cavity connection is required (plus two more at the module ends, which follow a different design).

*Frequency tuning* of each cavity is established by a mechanically driven length variation [6]. Since VSR operation may be frequently activated or suspended ("parking") by operational requests of BESSY II, a large tuning range of in total 1.1 MHz is needed in order to reach a sufficient frequency spread between strong and close-to-vanishing beam interaction. Such a wide-range tuning demands a significant cavity length variation of $\pm 0.6$ mm around a central on-resonance position.

*Acoustic decoupling* is needed in order to avoid big-sized acoustical entities out of two (or even more) cavities, which are able to oscillate mechanically with very low frequencies. Ambient excitation spectra tend to show the strongest acoustical excitations (which also may be generated by low frequency, e.g., 50 Hz, grid currents) below $\sim$100 Hz, a range that is much more likely in the acoustical mode spectrum of two-cavity chains instead of single cavities.

*Fabrication tolerances*, in particular with respect to small tilting angles (<0.2°) of the cavities' beam pipe flanges, need to be compensated. (This also applies to length deviations of the cavities, but those may exceed the affordable compensation range of the bellow and therefore shall be tolerated by means of dedicated dimensional adjustments of certain parts; in particular, the fundamental power couplers' mounting adaptors).

Slight mutual *cavity movements* during the mounting procedure should be allowed while the highly sensitive inner cavity and beam pipe volume are kept hermetically closed and are not affected by strong forces.

In Sec. II, the actual mechanical properties of CSB are described in further detail.

### 2. Beam impedance reduction options

Despite these needs, a bellow is an unwanted item in a synchrotron light source's beam pipe since its corrugated shape inevitably generates wakefields, a natural source of unfavorable beam impedance. This is of particular interest in view of the high beam currents typically seen in such kind of machines (≥300 mA in case of BESSY II). Four potential mitigation concepts are summarized in the following list:

*(a) Sliding contacts.*—It is a common practice to shield bellows from exposure to beam-excited fields by an inner layer of sliding contact springs (e.g., [7,8] and Refs. in both, [9,10], a comparison of different solutions in Ref. [11]). Such springs, which carry the mirror currents of the beam, cause only a very modest inhomogeneity of the beam pipe wall and therefore only contribute very weakly to the beam impedance. Spring contact shielding constructions are widely used and well established.

On the contrary, it was the key reason for the construction of CSB described in this paper that those sliding contacts need to be discarded in the neighborhood of SRF cavities since they are prone to release metallic particulates.

Such particulates with sizes of the order of some μm pose a severe operational risk to SRF cavities as they may generate local field emitters, unacceptably limiting the cavity's quality factor [12]. Therefore, it is commonly accepted that the avoidance of particulate contaminations of superconducting cavities during their preparative processing, assembly, and operation is paramount for reliable performance.

As a conclusion of this severe risk, it became a stringently followed construction rule for VSR/VSR DEMO not to apply any sliding contacts.

*(b) Spring connections.*—Searching for alternatives, it was analyzed whether flexible springlike metal strips bridging both ends of the bellow inside of it could serve as shielding elements. Since individual springs as a member of a shielding set are similar but not fully identical, such setups were found in own rf simulations to feature a very rich spectrum of resonant electromagnetic modes. This raises the risk of coincidence with prominent spectral components of the beam current, thus causing high Ohmic losses on singular springs with severe consequences of power deposition, outgassing, and possible thermal-induced mechanical breakdown. In view of the range of mechanical deformations hindering accurate numerical predictions, the approach was discarded after initial simulations.

*(c) Unshielded superconducting bellows.*—It was also investigated whether a shielding was required at all or whether niobium-made, superconducting bellows, which would be only negligibly heated by Ohmic losses, could be used. Unfortunately, such niobium-made bellows to the best of the authors' knowledge never reached operational reliability, even though some older [13] and also recent [14] investigations have been undertaken. However, even if such bellows were reliable, they would be a significant source of beam impedance and could not provide synchrotron light collimation, a secondary feature of importance (see Sec. IV). In Ref. [15] also an unshielded normal conducting setup was investigated, which utilized a stiff pipe section in between two short impedance-optimized bellows featuring only 2.5 convolutions. Using this arrangement, the beam energy deposition was successfully controlled whereas the local peak stress in the deforming segments found in simulations was understood as a potential limitation of the concept.

*(d) "Capacitive" shielding.*—In lack of options to shield the bellow with conductive connections, a known approach [16,17] is to establish a so-called capacitive shielding, which essentially means accepting a gap in the inner shielding surface, but keeping the gap width as small as possible and to establish opposing surfaces as large as affordable. Then, in a somewhat simplified description, the gap corresponds to a low capacitive impedance for all high-frequency components of the mirror currents accompanying the beam in the beam pipe wall while only low-frequency current components need to take the path along

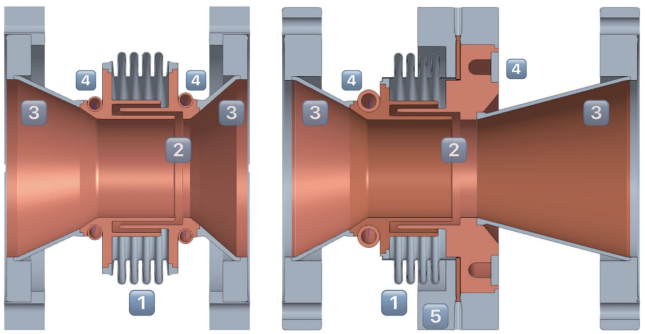


FIG. 2. Cross sections of CSB1 (left, a total length of 160 mm, upstream to the left) and CSB2 (right, 190 mm). Numbers indicate (1) stainless steel bellow, (2) combined shielding and collimating coaxial labyrinth made of OFHC copper, (3) stainless steel taper sections, copper coated, (4) cooling channels, (5) separating CF flange with copper gasket inlay.

the outer bellow. So, it was the aim of the construction to provide a wide-band low-impedance gap with low sensitivity against length variations (cf. Fig. 2).

#### *3. Length restriction*

Since VSR is intended to be installed in an already existing synchrotron light source, i.e., BESSY II at Helmholtz-Zentrum Berlin, the overall module length is limited by the existing magnet installation, giving a total available mounting length of 4.670 m. Within this length, it was a challenging task to fit the cryomodule together with beam pipe gate valves and combined taper/pumping/absorber sections (denoted as "Warm End Groups" [6,18]). The length limitation had severe impacts on the construction of all VSR parts contributing to real-estate length, including the CSB. VSR DEMO, featuring only two SRF cavities, would allow for a much more relaxed design, but by its developmental character, it is intended to demonstrate as many properties as possible needed later for VSR.

#### *4. Synchrotron light collimation*

A particular feature of the CSB is its inner cross-section reduction beyond the needs of the shielding itself, down to an inner diameter of 52 mm. This reduction will shadow downstream cavities from incoherent synchrotron light generated in the neighboring upstream dipole magnet. The illumination happens within a localized small surface of a few millimeters both in width and height, located on the outer collimator side at the height of the circulating beam (cf. Sec. V, Fig. 5). The radiated power was computed as 11 W [19], which would raise the load of the 2 K cooling circuit significantly even if homogeneously deposited in the SRF cavity (compare with the expected fundamental mode load of 26 W in case of 20 MV/m accelerating gradient). Even more severe, this deposition would be strongly localized making an appropriate cavity wall cooling at this certain spot questionable.

Even though a collimation is needed only in a small angular sector, a circular collimator shape was chosen for the sake of stronger cavity-cavity fundamental mode decoupling, field symmetry, and ease of production. The upstream taper of the CSB was lengthened as far as possible within the limited entire device length. This choice reduced its slope and thus reduced the power density on an increased illuminated surface.

#### *5. Active cooling needs*

On top of the synchrotron light deposition, the CSB is heated both by Ohmic dissipation of evanescent fundamental mode fields of the neighboring cavities and by wakefields. Detailed simulations (cf. Sec. IV) revealed an expected total thermal load of 32 W, which would far exceed the capabilities of conductive cooling through the flanges. Furthermore, any additional power loading on the 1.8 K cavity cooling system is rather unfavorable. Therefore, it was decided to equip the CSB with active He-cooling connected to the 5–8 K cooling system (denoted by the possible temperature range of the cooling media in biphase operation), which is foreseen in VSR/VSR DEMO as cooling for all components peripheral to the cavities. This is implemented by two (almost) circumferential cooling channels at both tapers.

With the active cooling, the inner taper ends of the CSB are kept at the 5–8 K temperature level, while the flanges connected to those of the cavities should stay as close to 1.8 K as possible. In order to reduce the static heat flow from the warmer central parts to the flanges the tapers are manufactured from stainless steel, which features a rather low thermal conductivity at cryogenic temperature levels. On the other hand, the taper should be of high electric conductivity to reduce the power deposition from the evanescent accelerating mode and also from wakefields. Therefore, the tapers are coated with a 20- to 25-μm thick copper layer, as an estimated best coating thickness in view of the conflicting demands of high electric, but poor thermal conductivity. The central parts of the CSB are made of massive oxygen-free high-conductivity (OFHC) copper with the exception of the stainless steel bellow, which has a brazed connection to the copper parts.

### C. Structure of investigations

The CSB concept was drafted in view of the demands described above. In particular, the length limitation imposes the development of a combined feature design while the restriction to avoid sliding contacts determined the use of a gapped shielding.

Several attempts of actual shaping were needed with the use of electrodynamic simulations to develop a design with low beam interaction. Here particular attention was devoted to nonpropagating modes resonating on harmonics of 250 MHz, which will be most prominent in a VSR beam pattern, featuring high-charge bunches every second bucket, i.e., every 4 ns. This affects in particular the low-frequency range with field patterns that do not couple to the HOM loads of the neighboring cavities.

For such modes, the CSB will operate as an unwanted cavity, dissipating wake power deposited by the beam in its own walls only. Since no other damping is available then, detuning is the only mean to avoid a resonant beam coupling. This demands a proper determination of resonant frequencies for any possible length extension, avoiding coincidence with 250-MHz harmonics under any circumstances.

Geometrically determined by cutoff frequencies, the regime of strongly localized modes ends above ~3.0 GHz. Fields of higher frequency can propagate through the beam pipes, the so-called cavity end-groups and the cavity waveguides toward the high-power water-cooled HOM loads, where they will be damped. Wake

analyses, performed up to 20 GHz, show the spectral richness of modes in the range above 3 GHz, which makes it impossible to detune all of them properly for all possible bellow length values, even though all of them appear sufficiently damped. This is attributed to the strong coupling provided by the five waveguide extensions and the single coaxial fundamental power coupler; a setup that also breaks up rotational symmetries, essentially for all modal types being able to propagate.

Even the low-frequency modes, which will hardly be excited by a densely populated VSR beam pattern, will start resonating in the case of a single bunch filling pattern. In the case of BESSY II, the bunch revolution time is 800.0 ns, which corresponds to a 1.25-MHz spectral line distance. For resonances in normal conducting structures, in particular with high-loss stainless steel walls, this is the order of resonant line width, which makes detuning impossible. Therefore, also the power deposition which is to be expected in single bunch operation was analyzed (cf. Sec. IV).

After completion of both the electromagnetic design and thermal computations (Sec. V.) and in view of the mechanical demands, the first CSB prototype (CSB1) was finally engineered and manufactured. Subsequent rf bench tests confirmed the expected mode frequencies as described in Sec. VI.

To install this prototype in BESSY II, a dedicated testing setup needed to be built with the primary purpose to match the existing beam pipe cross section with the 94-mm diameter circular flanges of the CSB. Several shapes of appropriate tapers were studied. As a result, a taper design equipped with strip lines serving as broadband damping elements was selected. This is described in Sec. VII. The setup allows varying the bellow length by a remote-controlled linear mover acting on one of the tapers and a second conventional spring-shielded bellow to compensate for the movement. The strip lines in the tapers are feeding in a total of 16 signals to rf loads, allowing also to analyze those outside the accelerator tunnel in time and frequency domain (even though limited by a severe cable damping up to ∼12 GHz). Such studies were undertaken, but results were—as expected—mainly dominated by the taper system. Therefore, they are not included in this paper.

CSB1 was operated in BESSY II for 16 months from August 2019 without severe complaints. The main issue was poor vacuum conditioning, which took several weeks, and even after that showed frequent spontaneous burstlike vacuum events, that did not affect machine reliability but remained unfavorable (cf. Sec. VIII).

This long-lasting conditioning issue was attributed to insufficient preparation of the inner surfaces of CSB1, which were not directly accessible after the final brazing. After dismantling CSB1 from BESSY II in early 2021, an inspection of the inner surfaces after the destructive cutting of the bellow revealed several impurities, which were very likely one of the causes of the observed behavior (cf. Sec. IX).

In order to mitigate the issue of poorly accessible surfaces, a redesign was developed which includes a flange connection between the two half-elements allowing for easy access and rigorous cleaning before mounting.

These modifications led to significantly improved vacuum performance seen in the beam test of CSB2, starting January 2022 (cf. Sec. XI).

## II. CSB1 AND CSB2 IN COMPARISON

CSB1 (Fig. 2, left) was the first prototype tested in BESSY II. It featured a full weld/braze connection closed on both sides of the bellow, which made the inner volume hard to access through the coaxial labyrinth. Wet ultrasonic cleaning was applied, followed by drying and clean room preparation, including pressurized N2-blowing, supported by particulate counting. This was driven to a level of particulate emission reduction nearby zero, as expected for a properly cleaned device. Nevertheless, there was no means to get direct contact to the surfaces of the inner labyrinth and the bellow. Later destructive dismantling revealed several surface impurities, likely to represent emitter locations (cf. Sec. IX).

In order to mitigate that significant design drawback, CSB2 (Fig. 2, right) was equipped with an additional flange in between the bellow and the downstream taper part. A dedicated combined gasket was used featuring rf contact lips at the innermost radius and a separated CF-style knife-edge vacuum gasketing zone close to the gasket's outer diameter; details to be reported in a separate publication. That allowed to prepare all inner surfaces of CSB2 prior to final mounting by ultrasonic wet cleaning, drying and bake-out, followed finally by pressurized N2-blowing and particulate counting.

CSB2 was designed to fit within the existing experimental taper setup (cf. Sec. VII), already used with CSB1, therefore being equipped with 94 mm diameter circular beam pipe connections. The additional inner flange and the need for sufficient space to insert all flange screws inevitably caused a modest length increase of 30 mm, mainly allocated in the downstream taper. In order to enlarge the cooling surface, the diameter of the upstream side cooling pipe was increased, while the downstream copper material block part got a newly designed cooling channel of U-shaped cross section, which was closed by a dedicated brazed surface element. Cleaning was done by wet ultrasonic, 120 °C drying of both parts open, followed by clean room mounting.

## III. MECHANICAL REQUIREMENTS AND PROPERTIES

The longitudinal compensation requirements were defined by the cavity length variations, which need to be

considered. Thermal shrinkage from room temperature down to 2 K for a 765 mm long niobium cavity is expected to reach 1.1 mm. The blade tuner is able to expand the cavity up to 1.2 mm, with an on-resonance position by design assumed in the centre of its range, i.e., a shortening of 0.5 mm referred to the warm unstressed length of the cavity. For mounting purposes, safety reasons and in view of a possible additional transversal mismatch (both axis offset and angular tilt) a possible compensation of $\pm 2$ mm ($\pm 3$ mm for CSB2) was demanded when procuring the stainless steel bellow.

Furthermore, it was required to withstand inner and outer over-pressurization (provided a stiff support in longitudinal direction) of 1.5 bar. These requirements led to the selection of a commercial standard-type bellow of 94 mm inner diameter, 122 mm outer diameter, 0.25 mm wall thickness with four convolutions, made out of stainless steel quality 1.4571, delivered by Witzenmann GmbH, Pforzheim, Germany.

Selecting an off-the-shelf commercial bellow was primarily motivated by the access to well tested and certified mechanical properties, which are regularly provided from the vendors for their standard sizes and types but are hard to collect for custom configurations.

## IV. CSB RF DESIGN

The rf design of the CSB followed three geometrical boundary conditions: The stainless steel bellow itself (i.e., its length including necessary weld connections, its convolution number and its inner and outer radius) was finally defined by the needed mechanical compensation capabilities. Second the largest possible inner beam pipe diameter was defined by the demand of proper synchrotron light collimation, assuming straight line of sights between the outermost point of synchrotron light generation (located in the closest upstream dipole magnet) and any possible point of illumination of the inner SRF cavity surfaces. This resulted in the choice of 52 mm inner diameter, giving a least safety margin. Third (as explained above) the design was dictated by the need of the shortest possible total device length.

The degrees of freedom to be optimized determine the shape of the inner labyrinth, i.e., the lengths and number of convolutions and filling of the volume inside of the inner below. There again geometric considerations got involved in order to cope also with minor angular deviations between the cavity flange planes, resulting in minimal radial distances in the labyrinth of 2 mm for the design geometry without tilt. Any design was tested numerically for its default length, 2 mm of extension and 2 mm of compression. Since the actual bellow shape is hardly be determined accurately enough for varying length, a purely longitudinal scaling of the bellow shape was applied as a first-order approximation.

The design was done in an experience-based trial-and-error strategy, with only the final outcome presented. Electromagnetic simulations were performed using the CSTStudio© suite [20]; in particular applying its eigenmode and (time domain) wakefield solvers. The latter is most suitable to identify frequencies of strong, resonancelike beam interactions within a broadband response, whereas the eigenmode solver more easily and with significantly lower numerical effort allows for tuning of nonpropagating modes confined to the bellow.

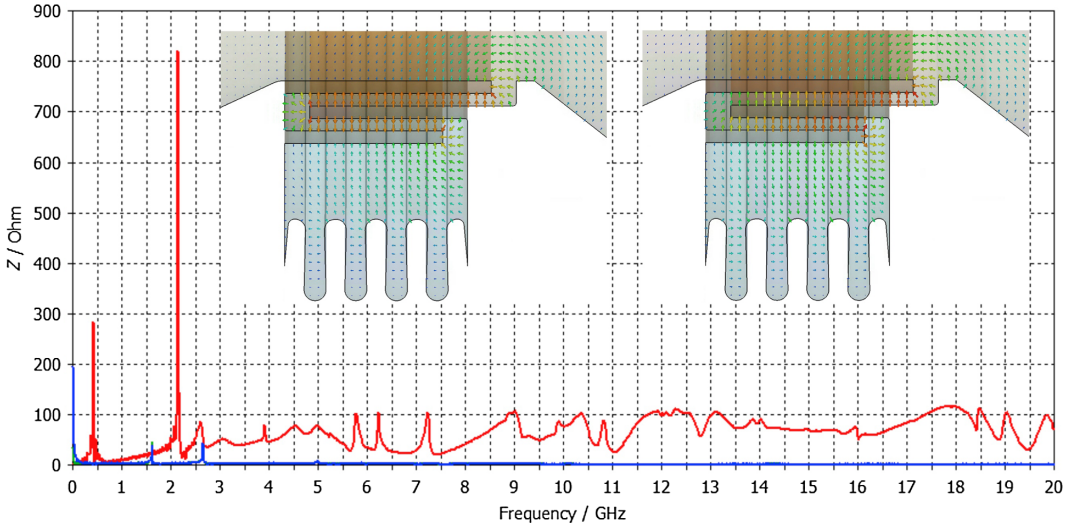


FIG. 3. Longitudinal beam impedance spectrum as simulated by the CSTStudio©-wakefield solver. The most relevant peaks were detected at 423, 2150, and (less prominent) 3912 MHz (cf. Fig. 4). Their accuracy is limited to the width of one frequency sampling interval of 20.5 MHz. The insets show details of the eigenmode solver E-field distribution results of the two modes of lowest eigenfrequencies. These modes are found at 422 MHz (left, $R/Q = 15.8\ \Omega$, no phase change along the labyrinth path) and 2155 MHz (right, $R/Q = 4.2\ \Omega$, phase shift of $\pi$ along the labyrinth path).

TABLE I. HOM power of the lowest three modes in the CSB.

| Frequency/GHz@$\Delta L$/mm | $R/Q/\Omega$@$\Delta L$/mm | $Q$ | $P_{\mathrm{loss}}$/W@20 mA | $P_{\mathrm{loss}}$/W@20 mA, steel only |
|---|---|---|---|---|
| 0.416@−2 | 14.3@−2 | | | |
| 0.422@0 | 15.8@0 | 497@0 | 6.70 | 5.52 |
| 0.423@+2 | 17.1@+2 | | | |
| 2.125@−2 | 4.3@−2 | | | |
| 2.155@0 | 4.2@0 | 1490@0 | 9.16 | 1.19 |
| 2.135@+2 | 4.2@+2 | | | |
| 3.976@−2 | 5.2@−2 | (simulation: bellow | | |
| 3.923@0 | 2.2@0 | without cavities) | | |
| 3.784@+2 | 2.2@+2 | | | |
| 3.928@0 | 0.734@0 | 1038@0 (with cavities, without loads) | 2.90 | 2.50 |

Figure 3 shows the beam impedance spectrum simulated up to 20 GHz for the bellow in its default length. It reveals two prominent resonances found at 422 MHz and 2.155 GHz together with a mostly broadband reaction in the high-frequency reaction. Eigenmode computations with length variations of ±2 mm resulted in minor frequency shifts below 20 MHz. The electrical fields of both modes are strongly localized between the coaxially folded counterparts of the shielding labyrinth, while they are much weaker in the outer, cavitylike volume delimited by the bellow. They also radiate in a similar manner into to the beam pipe volume. While for the fundamental mode (422 MHz), the entire labyrinth oscillates in phase, which is in direct analogy to a pure gap-bridging capacitor, the second one (2155 MHz) features a zero crossing close to the labyrinth's central corner. This also implies strong magnetic fields in that corner volume, which causes a nonmonotonous dependence of the frequency of mode 2 on the bellow length (cf. Table 1).

All higher modes are able to propagate toward the HOM loads attached to the cavity. The first example, found at 3.923 GHz, is shown in Fig. 4. In contrast to the modes of lower frequency, its fields, even though mainly localized in the bellow, reach the cavity and waveguide areas. Thus, their damping mainly happens in the water-cooled warm HOM absorbers attached to the cavity waveguides, so being by far less critical than the two fully localized lowest modes. All higher modes show even stronger field propagation; therefore, no narrow-banded peaks are found above 4 GHz in the beam impedance spectrum (cf. Fig. 3).

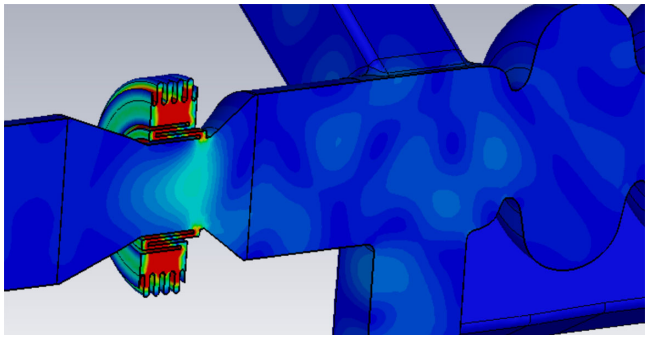

FIG. 4. (Unscaled) E-field power density of the third mode, found at 3.923 GHz, which extends into the waveguides.

Analysis of the field distributions simulated in the time domain revealed charge-normalized electrical field strengths in the labyrinth reaching up to 50 kV/(m nC). Bunch charges in BESSY II may reach 16 nC (single bunch operation with 20 mA of average current), then corresponding to peak field strengths of 800 kV/m. Those highly transient (few ps) peak fields are seen immediately after the bunch passage. Then a multitude of mostly fast decaying, overlaying modes is excited there, causing also a quick movement of the peak field locations in the entire labyrinth.

In order to estimate the power dissipated in the bellow, the beam-deposited power of the localized low-order modes is calculated. In the simplification of a fully homogeneous fill pattern with high bunch charges every 4 ns, only harmonic lines of 250 MHz would be excited. For several reasons (gap(s) in the fill pattern, special bunches with deviating charge, bunch charge jitter), this is not the case in practice, but the 250-MHz harmonics nevertheless remain strongly dominant in the power spectrum of a realistic fill pattern, being enhanced by ∼30 dB above the spectrum's base power level. Therefore, it is a valid technical approach to ignore the dissipation of any mode not oscillating (within its line width) in resonance with a harmonic of 250 MHz.

This consideration fails in case of a few-bunch or—most severe—a single bunch filling of the storage ring. Then this single bunch reappears every 800 ns, corresponding to a beam spectrum with harmonic lines every 1.25 MHz. Since this is clearly lower than the line width of modes in stainless-steel-bound resonators (which typically are about $Q \sim 1000$), the excitation cannot be avoided by detuning.

In order to calculate those losses, the mode loss factor $k_n$ will be used. It is defined as shown in Eq. (1) using its circular resonance frequency $\omega_n$, shunt impedance $R_n$, and quality factor $Q_n$:

$$k_n = \frac{\Delta U}{q^2} = \frac{\omega_n}{2}\frac{R_n}{Q_n}. \tag{1}$$

Rewriting the bunch charge $q$ using the time-average beam $I_{\mathrm{beam}}$ and the revolution time $\Delta t$ (which in case of a single bunch filling is equal to the time in between repeated passes):

$$q = I_{\mathrm{beam}}\Delta t \tag{2}$$

and similarly the energy loss per turn in terms of a time-averaged deposited power $P_{\mathrm{loss},n}$:

$$\Delta U = P_{\mathrm{loss},\,n}\Delta t \tag{3}$$

allows to combine Eqs. (1)–(3) in order to calculate the time-averaged beam deposited power of a certain mode:

$$P_{\mathrm{loss},n} = \frac{\omega_n}{2}\frac{R_n}{Q_n} I^2_{\mathrm{beam}}\Delta t. \tag{4}$$

The mode-characteristic quantities $\omega_n$, $R_n$, and $Q_n$ of eigenmodes are numerically accessible from the CST eigenmode simulations, $I_{\mathrm{beam}}$ and $\Delta t$ are well known.

Only in case of the two nonpropagating modes, it is assumed that their deposited power is also (fully) dissipated in the CSB, while in case of all other modes, the significantly stronger damping located in the HOM absorber gives reason for the simplification that their losses are not accounted in the CSB for estimating the cooling power demands in the case of single bunch operation. Table I summarizes the calculated power estimates (including a third mode (cf. Fig. 4) which is propagating but was simulated as a worst-case situation without HOM loads). Whereas modes 1 and 3 show their main losses in the stainless steel part, mode 2 has its dominant losses in the copper labyrinth.

A second source of power losses originates from outward leaking fundamental mode fields of the neighboring cavities. Those were calculated by eigenmode computations in a two-cavity-setup as 1.46 W in case of 20 MV/m accelerating field strength, 0.35 W of which is deposited in the stainless steel part.

## V. CSB THERMAL DESIGN AND SIMULATION

The main concern in the thermal layout of the CSB is the reduction of the thermal power flow toward the cavities, which are designed to operate at 1.8 K, implying an extremely poor cooling efficacy and a limited cooling power budget. Therefore, active cooling was designed, which is directly attached to the innermost copper-made parts and is connected to the 5–8 K biphase cooling circuitry.

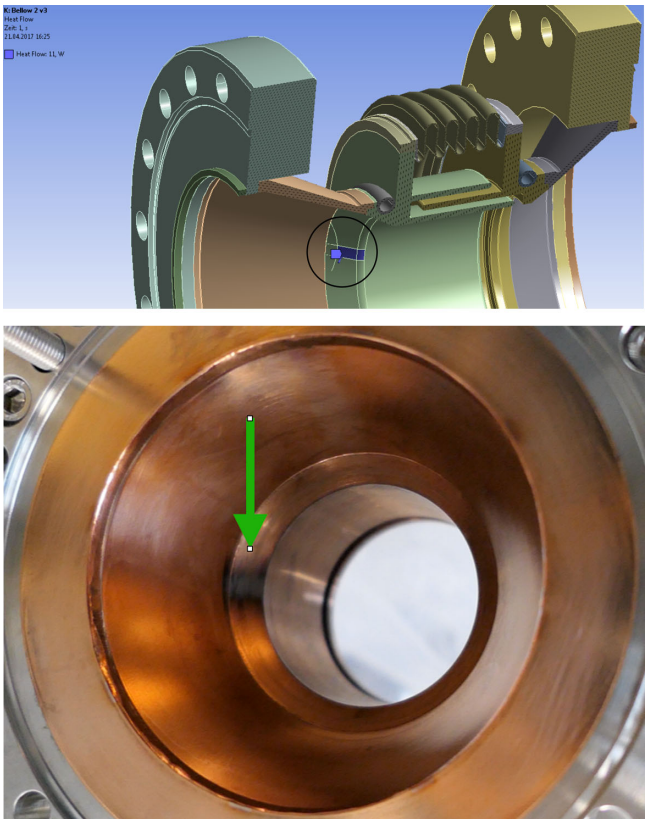

FIG. 5. Synchrotron light impact zone as assumed in the thermal simulation (above, encircled) and discoloration found very close to the estimated place after operating and dismantling CSB1 in the estimated area (below, green arrow).

Thermal loads were derived from the HOM eigenmode simulations and weighted for the 20-mA single bunch operation as the worst case, also considering the spatial distribution of the main material compartments. In total, they sum up to 18.8 W. Additionally 1.5 W caused by fundamental mode heating was considered.

Furthermore, a rectangular spot illuminated by a light cone of $2 \times 2$ mm$^2$ cross section and 11 W of synchrotron power was assumed, following draft raytracing estimations (cf. Fig. 5). Therefore, a total heat load of 31.3 W was assumed in the thermal simulation. A fixed temperature boundary kept at 2.0 K was assumed on both flanges and a convective boundary in both pipes toward a 5 K media with a thermal resistance of 0.002 W/(mm$^2$ K). Those were assumed as the only cooling mechanisms, neglecting radiation effects. Simulations were performed with the stationary thermal solver of the ANSYS suite [21].

These assumptions led to a temperature distribution as shown in Fig. 6. The stainless steel bellow reaches remarkably high values of above 130 K, whereas the highly conductive copper parts show a quite homogeneous

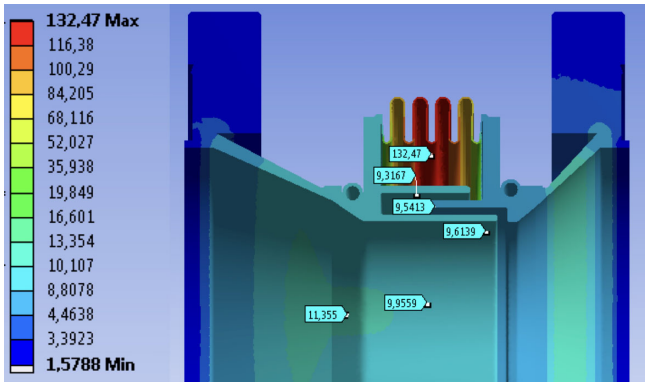


FIG. 6. Temperature distribution in K as simulated with a total thermal load of 31.3 W.

temperature distribution around 10 K with the exception of the area around the synchrotron light impact area, where 11.4 K was reached at maximum. The stainless steel flanges with their extremely poor heat conductivity at cryogenic temperatures work properly as strong thermal resistors, keeping the total heat flux toward the cavities lower than 4 W. Similarly, the peripheral parts of the stainless steel bellow, which are well cooled by their connection to the massive copper parts, are of very low heat conductivity and thus confine the extension of the hot area in the middle of the bellow (cf. Fig. 6).

## VI. CSB1 RF BENCH FREQUENCY CHECK

The CSB1 prototype was equipped with provisional closing end plates and a central capacitive antenna in order to check the expected rf properties using a network analyzer [18]. The simulation needed to incorporate the end plates, which are not present in any other operational conditions. The two most relevant and four other modes were found with the bellow adjusted to its default length in good mutual agreement, with deviations between simulation and experiment: −6.7, −20.3, +15.6, −18.7, +47.0, +2.4 MHz, sufficient to confirm the model validity (cf. [18], Fig. 4).

## VII. BEAM TEST SETUP

In order to install CSB1 (and later also CSB2) in the BESSY II storage ring, a testing setup was developed, built, installed, and operated, with the main purpose of adapting the polygonal beam pipe cross section used in BESSY II to the circular 94-mm diameter circular beam pipe flanges of both CSB1 and CSB2. Geometrically, the setup itself represents a "parasitical" cavity capable to support a large set of unwanted modes. Several taper designs were investigated, reaching from long beam pipes of large cross section (suffering from a very dense spectrum of longitudinal modes) to very short and steep shapes (generating unfavorably strong beam impedance contributions). A mock-up of two cavity end groups aside the CSB, which would resemble the rf conditions in a real VSR setup more closely, was discarded because of the very severe efforts needed.

As a result, wakefields were mitigated as far as possible using tapers of the moderate slope, which are equipped with four stripline-shaped broadband HOM couplers, also giving access to rf signals extracted from the setup through the pair of feedthroughs connected to each stripline (cf. Fig. 7). Field patterns, which are extended into the taper parts, will experience significant damping, while modes localized in the bellow are coupling only very

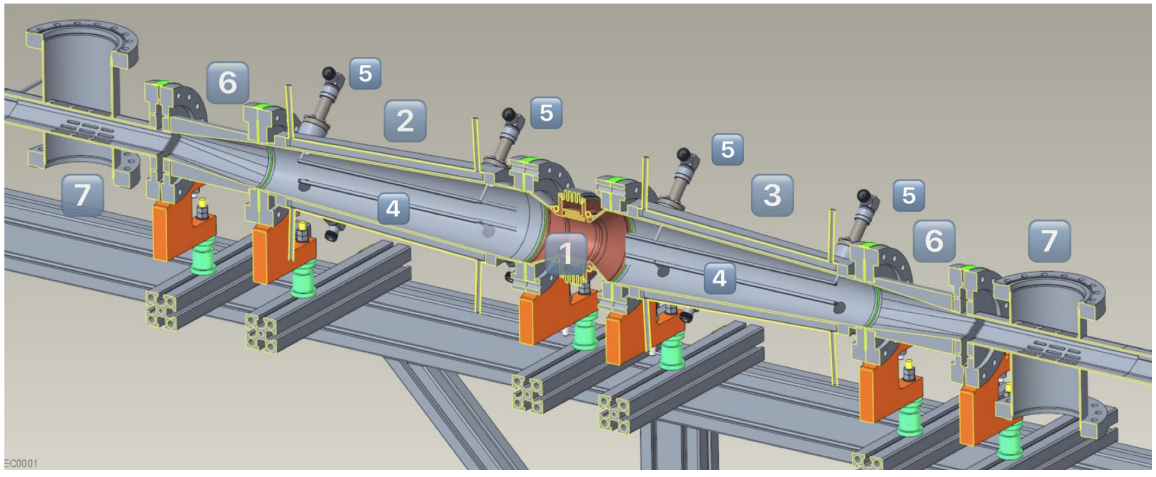


FIG. 7. HOM-damped taper setup (in cross-sectional view) used to install CSB1/CSB2 into the BESSY II storage ring. The bellow (1) is mounted in the middle in between two conical inner taper parts (upstream (2), downstream (3)), which are equipped with stripline couplers (4). Those are connected via feedthroughs (5) and cables to external loads (not shown). Two intermediate pieces (6) adopt for the polygonal BESSY II beam pipe cross section. Two pumping ports (7), both carrying a pair of getter pumps, downstream also a pressure gauge (not shown) complete the setup.

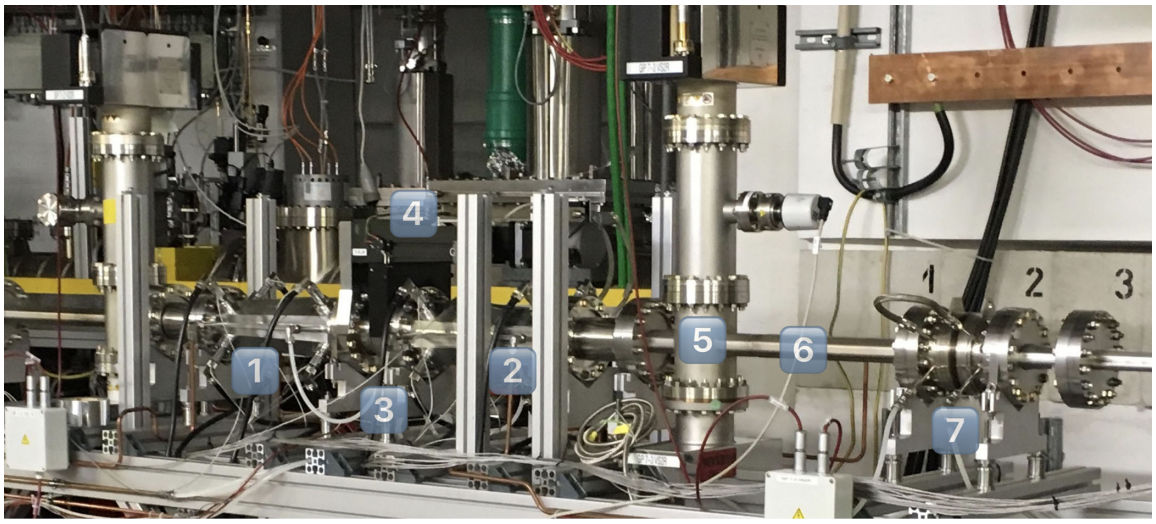


FIG. 8. The installation of the CSB1/CSB2 test setup in the BESSY II storage ring. The taper setup (1), (2) keeps the CSB (3) in the middle, where a linear mover (4) can adjust its length remotely controlled. The downstream taper (2) together with the attached pumping dome (5) and beam pipe (6) move as a whole; length compensation is provided with a conventional bellow (7).

weakly to the striplines, which resembles the situation in the VSR module.

Each of the 16 feedthrough ports was connected to a coaxial cable of ∼52 m length, therefore absorbing most of the deposited wakefield power (measured damping −13.6 dB@1 GHz, −37.6 dB@6 GHz) and transferring the signal to a terminating coaxial load located on top of the BESSY II radiation shield.

In order to control the bellow length, a linear mover was mounted on top of the bellow, attaching both flanges. The mover was driven by a stepper motor, regularly operated with 10 μm step sizes, and remotely controlled. The movement was limited by hard switches to a range of ±2 mm, such protecting the bellow. The downstream taper together with its pumping port and a piece of BESSY II standard beam pipe were able to move together on a sliding mount. Further downstream a conventional spring-shielded bellow was used to compensate for that movement (cf. Fig. 8).

Temperatures of the taper housing and all feedthroughs were measured with PT100 sensors attached from the outside using adhesive strips. A special flat PT100 sensor shape was needed also to monitor the temperature of the bellow convolutions, which was not available for all experiments but starting from early November 2019 until the dismantling of CSB1.

Both the bellow's cooling pipes and the inner taper pieces, which are equipped with two water cooling channels, were connected with the central supply of cooling water, entering the devices at ∼30 °C. No efforts were made to measure the thermal energy balance since the bellow was operated in air and temperature-dependent thermal conductivities like Ohmic resistances are hardly comparable with later cryogenic conditions. Nevertheless, the temperature data are useful for comparative assessments of different operational conditions—in particular different bellow length adjustments and beam fill patterns. They were also intended for the purpose of machine protection, albeit critical values never came within reach.

Vacuum conditions were analyzed primarily using the data of a pressure gauge (internally and in the viewgraphs denoted as "VMC3VS2R," Pfeiffer Vacuum PKR261, measurement range $>5 \times 10^{-9}$ mBar) attached at the downstream pumping port; getter pump currents and readouts of a second pressure gauge at the upstream end of the installation were also monitored and saved. The observation of the vacuum quality revealed the most critical aspect of the CSB1 construction and gained therefore the highest attention.

## VIII. BEAM TEST PERFORMANCE OF CSB1

After BESSY II's 2019 summer shutdown, during which CSB1 was installed into the storage ring within the test setup described, beam operation resumed beginning of September 2019. The machine current was raised stepwise over a period of about 2 months before reaching the full current of 300 mA to commission a total of three new components, one of them being the CSB1 (cf. Fig. 9). During that time, a slow overall pressure reduction was observed. By monitoring the pressure readout, it was possible to identify at least four different types of reactions:

*(a) Triggered spikes* clearly coincide with either a change of the beam filling pattern (cf. Fig. 10 leftmost) or a mechanical length variation (cf. Fig. 11). Such spikes appear in a wide range of heights and may extend in rare cases up to or even beyond 1 order of magnitude. Since they decay fast within $\sim 10^1 - 10^2$ s they are attributed to sudden and singular evaporation events like blowing ups of singular field emitters.

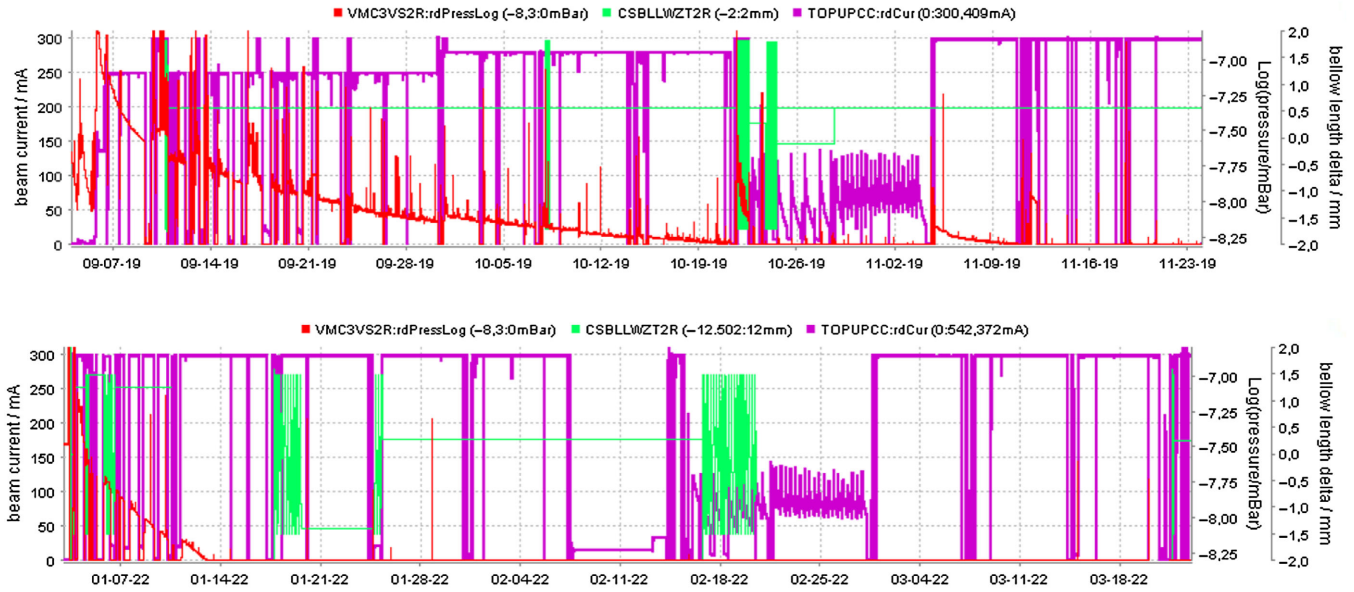


FIG. 9. Displays of data retrievals from the BESSY II archiver ("Log" denotes decadic logarithm, also in Figs. 10–15). Top: Vacuum conditioning history (red) of CSB1 after pumping starts until reaching the lower measuring limit ($5 \times 10^{-9}$ mBar) of the pressure gauge after ~80 days. Commissioning of two other components and the CSB1 gave reason for a stepwise increase of the machine current (magenta). The reaction on variations of the bellow length (green) was tested in three dedicated periods. Bottom: Similar graph for CSB2, which reached $5 \times 10^{-9}$ mBar already after 10 calendar days, BESSY II being operated (with some interruptions) with 300 mA from the beginning.

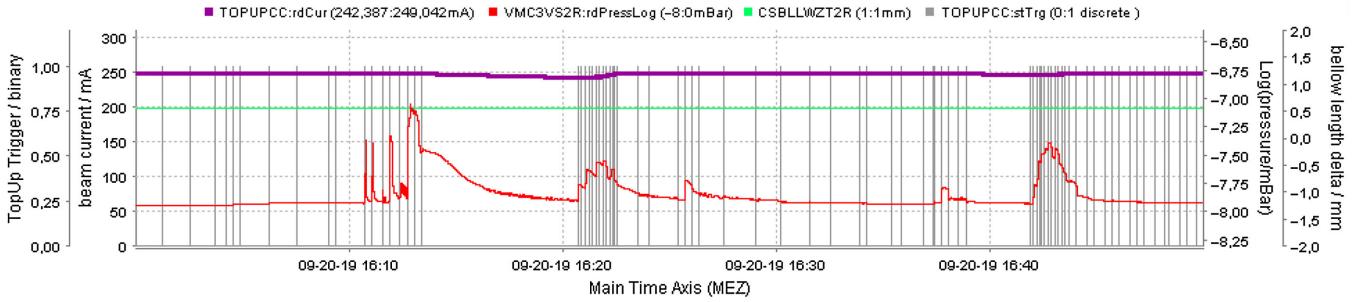


FIG. 10. CSB1 pressure gauge readout (red), beam current (magenta), and topup injection trigger times (light gray) (no bellow movements—green). Additional injections may trigger short pressure bursts (leftmost spikes, decay times ~$10^1$ s), processes of slow conditioning (~$10^2$ s), and also sudden pressure decrease events as shown here for a sample time interval.

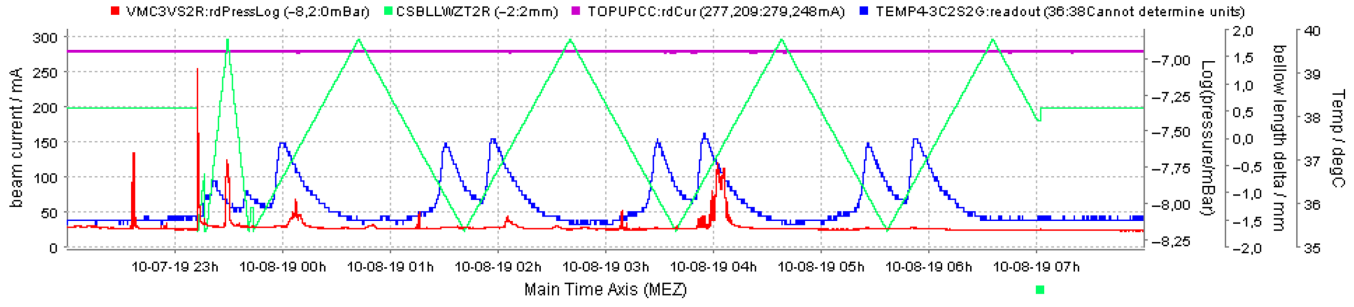


FIG. 11. CSB1 pressure gauge (red) and temperature (blue, °C) readout during cyclic length variation (green). A clearly length-correlated temperature signal is observed during the entire experiment, while the pattern of the pressure reaction disappeared after a strong peak at the beginning of the third long cycle, indicating a conditioning process.

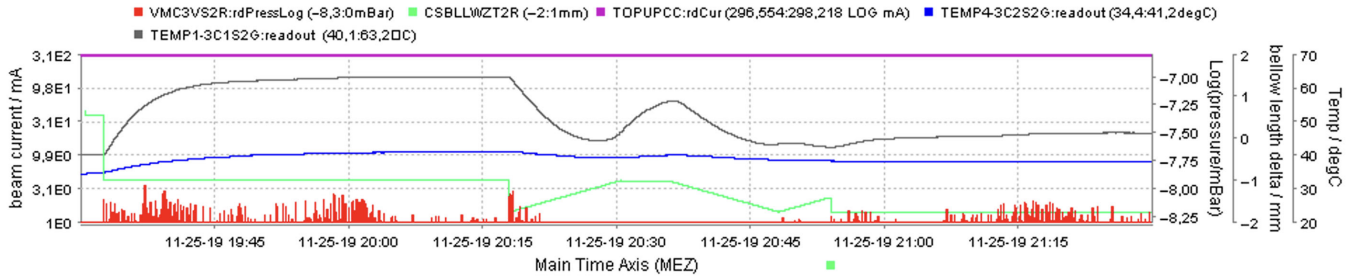


FIG. 12. Highest bellow convolution temperature (black, maximum of 63.2 °C, other color coding like Fig. 11) measured during the CSB1 installation time, caused by tuning the bellow to its length with the strongest vacuum activity observed previously.

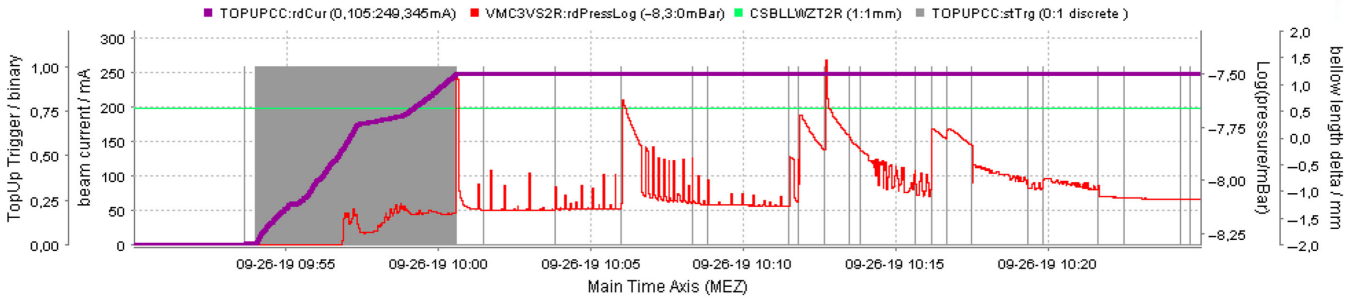


FIG. 13. Oscillatory, slowly decaying, and suddenly interrupted pressure signals observed with CSB1 (color coding like Fig. 10).

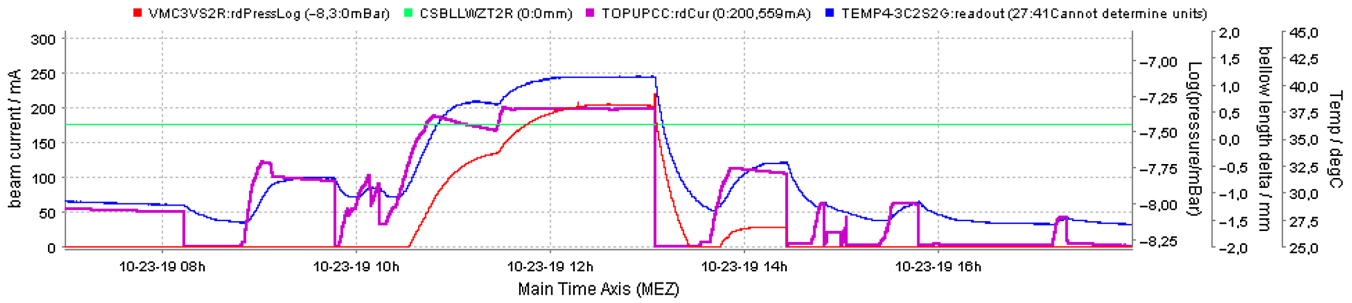


FIG. 14. CSB1 pressure gauge readout (red), temperature (blue, °C) readout during so-called "low-alpha" operation of BESSY II with shortened bunch lengths (~9 ps), first successfully tested on October 23, 2019, with up to 200-mA total beam current, which marks an all-time record for BESSY II current in "low-alpha" operation.

In contrast to its function as a fast trigger, mechanical tuning was also observed as a reason for longer-lasting periods of vacuum activity, typically also accompanied by significant heating (cf. Fig. 12 for the most extreme heating observed at CSB1). These conditions are understood as mutually self-amplifying (cf. c) and driven by strong, most likely resonant electromagnetic fields in the bellow.

*(b) Slowly decaying and oscillatory pressure* (cf. Fig. 13) is like the spikes characterized by a very steep increase, while showing in contrast a distinctively slower decay, which also may oscillate fast between upper and lower envelope curves. Remarkably, such activity periods often suddenly stop synchronous to a beam pattern change indicated by a topup injection trigger signal. The behavior may be interpreted as ignition (and extinction) of glowing discharges, but further evidence on this is lacking.

*(c) Temperature-correlated* pressure increase (cf. Fig. 14) is a phenomenon commonly understood as the ambient surface outgassing being accelerated by the raise of the housing temperatures; pressure directly follows the temperature signal. After the initial phase of conditioning, such a phenomenon is observed most prominently if special conditions give the reason for elevated temperatures. In Fig. 14, such increased temperatures were caused by additional bunch shortening during the so-called low-alpha operation of BESSY II. Shorter bunches generate more high-frequency wakefields also raising losses because of the increase of surface resistance with increasing frequency.

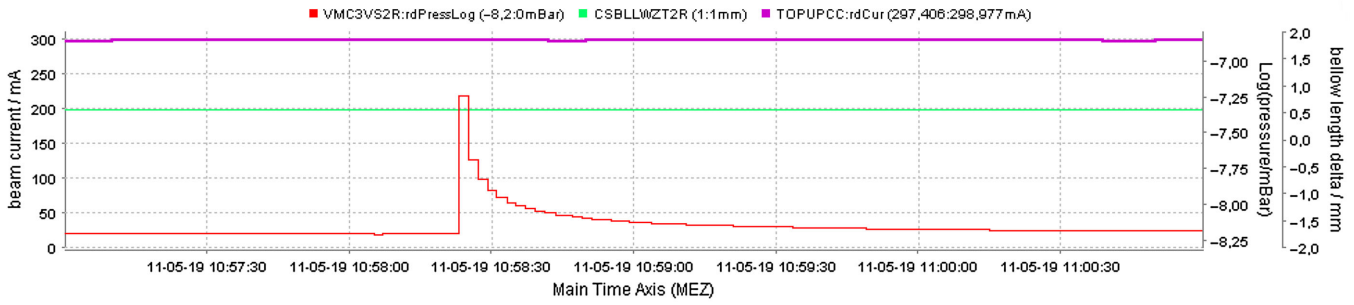


FIG. 15. Singular spike of roughly 1 pressure magnitude (red) as an example of events occasionally (few per month) observed both with the setups of (here) CSB1, CSB2 and also in the replacement straight (used after the dismantling of CSB1 and before installation of CSB2). There is no clear event trigger like a bellow movement (green), temperature (light blue), or fill pattern change (e.g., initiated by a topup injection—gray) observable.

*(d) Nontriggered spikes* (cf. Fig. 15), understood as singular events without any clear correlation to an initiating process, were observed seldom ($<1$/week), but persistently. That happened both during the installation periods of CSB1 and CSB2 and also during the installation of a replacement beam pipe (January to December 2021). The latter reveals such sparse events as being not specific to the CSB construction.

## IX. INSPECTION OF CSB1'S INNER SURFACES

Because of the unsatisfactory vacuum performance, CSB1 was destructively split after dismantling it from BESSY II at the end of 2020 in order to inspect its inner surfaces. This was done by cutting the stainless steel bellow close to the downstream end plate. The volume captured inside had its only opening through the coaxial labyrinth, which allowed for a wet cleaning but hindered all flow processes like drying and pressurized gas blowing and made a visual inspection impossible.

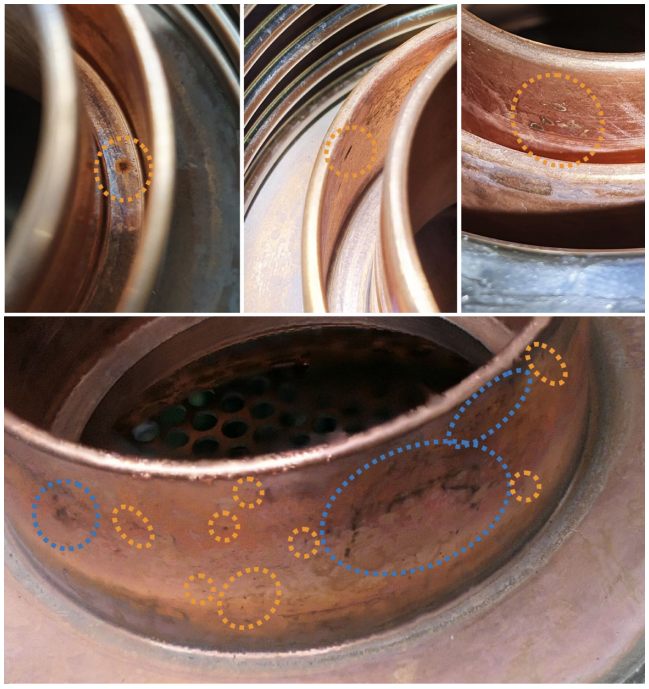

FIG. 16. Spot-sized (orange) and extended (blue) discolorations found on the labyrinth surfaces of CSB1 after cutting.

The surfaces of both parts showed after opening significant amounts of impurities and deposits. In particular, a large number of dark spots and also a few extended areas of dark brown to black color were identified (cf. Fig. 16). The distribution of visual impurities gave no clue to specific localizations. Also, accidentally close approximations of opposing surfaces were excluded by the rigidity of the linear mover unit, keeping both sides aligned on the axis. To a certain extent, uneven brazing remnants, turning tracks, and a single scratch were also found, which were out of the expected manufacturing quality.

This overall picture was estimated as very likely reasoning for strong outgassing without particular analysis of certain spots.

## X. OPERATIONAL EXPERIENCE WITH CSB2

At the beginning of January 2022, CSB2 (cf. Fig. 17) came into operation in BESSY II [22]. As described above, the experiment reused the taper, pumping, and sensor setup. CSB2 incorporated the new central flange, allowing to split the device for inspection and cleaning, which was rigorously performed in advance (wet ultrasound cleaning, 120 °C drying, clean room closing with particulate release control, mounting under a temporary local clean room).

It was immediately possible to raise the machine current to the nominal value of 300 mA. Vacuum conditioning was much faster than that of CSB1 (cf. Fig. 9) and reached the lower measurement limit after 10 calendar days with some machine downtime for other commissioning reasons. About 20 minor and 2 strong pressure spike events were counted at that time. Initial bellow length variations triggered no events (cf. [22], Fig. 2). From January 17 to 19, length cycling was tested which revealed a very moderate temperature variation but triggered no pressure events.

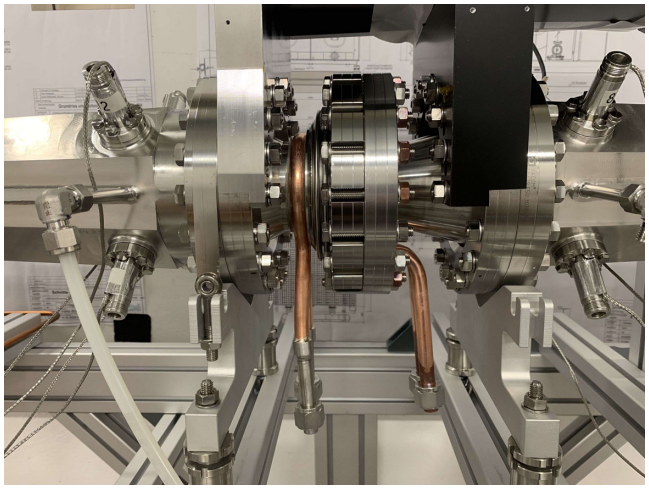

FIG. 17. CSB2 prepared for installation in BESSY II.

CSB2 experienced the first single bunch operation on January 24 with 20 mA. In the very initial filling a short conditioning of about 20 min was seen in the pressure signal without any further reaction (cf. [22], Fig. 3). From February 7 to 13, BESSY II was operated with a 15-mA single bunch, followed by 1 day with 32 mA distributed to four equally spaced bunches (so-called "few-bunch-operation") without any observable pressure reaction at CSB2 (cf. Fig. 9). Same holds for the 12 days period starting at 16th February of low-alpha operation, which also included 4 days of length cycling (cf. [22], Fig. 4).

A rare experiment, raising BESSY II's current to 350 mA, was conducted on March 22 (cf. [22], Fig. 5). Individual bunch charges were kept, but about half of the regular pause of 100 buckets was additionally filled. This interestingly lowered the taper temperature, which can be explained by the shift of spectral beam current components away from rf resonances of the setup. Again, no pressure reactions were seen. On the 2nd of May, the current was held even higher at 400 mA for about 4.5 h, again without any pressure and only very slight temperature reactions.

Therefore, CSB2 successfully mastered all kinds of regular (up to 400 mA) and special (20 mA single bunch, 32 mA few-bunch, 100 mA low-alpha) operation modes of BESSY II.

## XI. CONCLUSIONS AND OUTLOOK

The collimating shielded bellow is the first VSR component that was successfully integrated into BESSY II and tested during all kinds of beam operations.

So far, there have been two iterations of this component. CSB1 already showed that integration into the BESSY II ring was possible but revealed unexpected difficulties relating to vacuum conditioning that were successfully overcome with the improved split design of CSB2.

This completed a development sequence including mechanical, rf and thermal design, rf bench tests, design, construction, and implementation of a beam testing setup, and extensive beam testing as far as it is possible in a noncryogenic environment.

The VSR DEMO module which is recently under construction will allow to test the interoperability of CSB in its third generation with SRF cavities in cryogenic operation, ideally installed in BESSY II.

## ACKNOWLEDGMENTS

This work is supported by grants from the Helmholtz Association.

[1] G. Wüstefeld, A. Jankowiak, J. Knobloch, and M. Ries, Simultaneous long and short electron bunches in the BESSY II Storage Ring, in *Proceedings of the 2nd International Particle Accelerator Conference, San Sebastián, Spain* (EPS-AG, Spain, 2011), THPC014, pp. 2936–2938, http://accelconf.web.cern.ch/ipac2011/papers/thpc014.pdf.

[2] *Technical design study BESSY VSR*, edited by A. Jankowiak, J. Knobloch, P. Goslawski, and N. Neumann (Helmholtz-Zentrum, Berlin, Germany, 2015), 10.5442/R0001.

[3] A. Velez and H.-W. Glock, Superconducting radio-frequency for high-current CW applications, in *Synchrotron Light Sources and Free-Electron Lasers*, 2nd ed., edited by E. J. Jaeschke, S. Khan, J. Schneider, and J. B. Hastings (Springer Nature, Switzerland, 2019), 10.1007/978-3-319-04507-8_59-1.

[4] F. Glöckner, F. Pflocksch, D. Wolk, D. Böhlick, V. Dürr, A. Frahm, M. Bürger, N. Wunderer, J. Knobloch, and A. Velez, The VSR DEMO Module design—a spaceframe-based module for cavities with warm waveguide HOM absorbers, in *Proceedings of 20th International Conference on RF Superconductivity, SRF2021, East Lansing, MI* (JACoW, Geneva, Switzerland, 2019), pp. 233–236, 10.18429/JACoW-SRF2021-MOPTEV013.

[5] E. Sharples-Milne, V. Dürr, J. Knobloch, S. Schendler, A. Velez, and N. Wunderer, The 1.5 GHz Coupler for VSR DEMO: Final Design studies, Fabrication Status and Initial Testing Plans, in *Proceedings of 20th International Conference on RF Superconductivity, SRF2021, East Lansing, MI* (JACoW, Geneva, Switzerland, 2019), pp. 652–656, 10.18429/JACoW-SRF2021-WEPTEV009.

[6] N. Wunderer, V. Dürr, A. Frahm, H.-W. Glock, F. Glöckner, J. Knobloch, E. Sharples-Milne, A. Tsakanian, A. Velez, M. Bonezzi, A. D'Ambros, R. Paparella, J. Guo, J. Henry, and R. Rimmer, VSR DEMO cold string: Recent developments and manufacturing status, in *Proceedings of 20th International Conference on RF Superconductivity, SRF2021, East Lansing, MI* (JACoW, Geneva, Switzerland, 2021), pp. 647–651, 10.18429/JACoW-SRF2021-WEPTEV008.

[7] Y. Suetsugu, K. Ohshima, and K. Kanazawa, Design studies on a vacuum bellows assembly with radio frequency shield for the KEK B factory, Rev. Sci. Instrum. **67**, 2796 (1996).

[8] Y. Suetsugu, M. Shirai, and K. Shibata, Possibility of comb-type rf shield structure for high current accelerators, Phys. Rev. ST Accel. Beams **6**, 103201 (2003).

[9] N. R. Kurita, A. Kulikov, M. Nordby, and J. Corlett, Final design and manufacturing of the PEP-II high energy ring arc bellows module, *Proceedings of the Particle Accelerator Conference, Vancouver, BC, Canada, 1997* (IEEE, New York, 1997), pp. 3639–3641.

[10] S. Tomassini, F. Marcellini, P. Raimondi, and G. Sensolini, A new RF shielded bellows for DAΦNE upgrade, in *Proceedings of the 11th European Particle Accelerator Conference, Genoa, 2008* (EPS-AG, Genoa, Italy, 2008), TUPP074, pp. 1706–1708.

[11] H. O. C. Duarte, R. M. Seraphim, T. M. Rocha, A. R. D. Rodrigues, and P. P. S. Freitas, Design review of bellows RF-shielding types and new concepts for SIRIUS, in *Proceedings of the 10th International Particle Accelerator Conference, IPAC-2019, Melbourne, Australia* (JACoW, Geneva, Switzerland, 2019), pp. 53–56, 10.18429/JACoW-IPAC2019-MOPGW001.

[12] R. Geng, A. Freyberger, R. Legg, R. Suleiman, and A. S. Fisher, Field emission in SRF accelerators: Instrumented measurements for its understanding and mitigation, in *Proceedings of 6th International Beam Instrumentation Conference, IBIC2017, Grand Rapids, MI* (JACoW, Geneva, Switzerland, 2017), TH1AB1, pp. 470–477, 10.18429/JACoW-IBIC2017-TH1AB1.

[13] L. Turlington, J. Brawley, R. Manus, S. Manning, S. Morgan, G. Slack, and P. Kneisel, Development of a Niobium Bellows for Beamline Connections, United States (2003), https://www.osti.gov/biblio/822206.

[14] R. Rimmer, JLAB (private communication).

[15] G. Wu, R. Rimmer, J. Feingold, H. Wang, J. Mammosser, G. Waldschmidt, A. Nassiri, J. H. Jang, S. H. Kim, K.-J. Kim, and Y. Yang, Low impedance bellows for high-current beam operations, in *Proceedings of the 3rd International Particle Accelerator Conference, New Orleans, LA, 2012* (IEEE, Piscataway, NJ, 2012), WEPPC042, pp. 2303–2305.

[16] Y. Zhao and H. Hahn, Concepts for capacitively RF-shielded bellows in cryogenic structures, Brookhaven National Laboratory, Upton, NY, Report No. C-A/AP/#141, 2004.

[17] Y. Suetsugu, K. Kanazawa, N. Ohuchi, K. Shibata, and M. Shirai, Application of comb-type RF shield to bellows chambers and gate valves, in *Proceedings of the 21st Particle Accelerator Conference, Knoxville, TN, 2005* (IEEE, Piscataway, NJ, 2005), pp. 3203–3205, 10.1109/PAC.2005.1591413.

[18] H.-W. Glock, V. Dürr, F. Glöckner, J. Knobloch, M. Tannert, A. Velez, D. Wolk, N. Wunderer, J. Guo, H. Wang, and R. Rimmer, Progress of the BESSY VSR cold string development and testing, in *Proceedings of 10th International Particle Accelerator Conference, IPAC-2019, Melbourne, Australia* (JACoW, Geneva, Switzerland, 2019), pp. 1434–1436, 10.18429/JACoW-IPAC2019-TUPGW019.

[19] M. Ries, HZB (private communication).

[20] Simulia CST studio Suite Vers. 2019.05, Dassault Systems Deutschland GmbH.

[21] ANSYS vers. 2017, ANSYS, Inc., 275 Technology Drive, Canonsburg, PA 15317.

[22] H.-W. Glock, V. Dürr, F. Glöckner, J. Knobloch, M. Ries, and A. Velez, Operational experience with the improved VSR DEMO collimating shielded bellow in BESSY II, in *Proceedings of the 13th International Particle Accelerator Conference, IPAC-2022, Bangkok, Thailand* (JACoW, Geneva, Switzerland, 2022), pp. 2497–2500, 10.18429/JACoW-IPAC2022-THPOST025.